CONF-950304--5

ATMOSPHERIC CORROSION MONITORING AT THE U.S. DEPARTMENT OF ENERGY'S OAK RIDGE K-25 SITE

Mukund Rao*
Technical Division
The Oak Ridge K-25 Site
Oak Ridge, TN 37831-7272

ABSTRACT

Depleted uranium hexafluoride (UF_6) at the U.S. Department of Energy's K-25 Site at Oak Ridge, TN has been stored in large steel cylinders which have undergone significant atmospheric corrosion damage over the last 35 years. A detailed experimental program to characterize and monitor the corrosion damage was initiated in 1992.

Large amounts of corrosion scale and deep pits are found to cover cylinder surfaces. Ultrasonic wall thickness measurements have shown uniform corrosion losses up to 20 mils (0.5 mm) and pits up to 100 mils (2.5 mm) deep. Electrical resistance corrosion probes, time-of-wetness sensors and thermocouples have been attached to cylinder bodies. Atmospheric conditions are monitored using rain gauges, relative humidity sensors and thermocouples. Long-term (16 years) data are being obtained from mild steel corrosion coupons on test racks as well as attached directly to cylinder surfaces. Corrosion rates have been found to be intimately related to the times-of-wetness, both tending to be higher on cylinder tops due to apparent sheltering effects. Data from the various tests are compared, discrepancies are discussed and a pattern of cylinder corrosion as a function of cylinder position and location is described.

Keywords: atmospheric corrosion, pitting, mild steel, corrosion probes, time-of-wetness, corrosion coupons, sheltering, condensation, UF_6 cylinders.

---

*Midwest Technical Inc., under subcontract 1BK-02268C with Martin Marietta Energy Systems Inc., which manages the Oak Ridge K-25 Site for the U.S. Department of Energy, under contract DE-AC05-84OR21400.

INTRODUCTION

The U.S. Department of Energy's K-25 Site at Oak Ridge, TN produced enriched uranium using the gaseous diffusion process until it was permanently shut down in 1987. Depleted uranium hexafluoride (UF_6) from the process has been stored at the site mainly in 10- and 14- ton mild steel (ASTM grades A285 and A516) cylinders stacked in outdoor yards. The cylinders typically are 4 feet (1.2 m) in diameter and 10 to 12 feet (3 to 3.65 m) long with wall thicknesses of 5/16" (8 mm), and are designed, manufactured and maintained in accordance with the ASME Boiler and Pressure Vessel Code for unfired pressure vessels. A large number of the approximately 5000 such cylinders, some of which have been in storage for periods up to 35 years, have undergone significant atmospheric corrosion damage during storage. Since the cylinders are expected to remain in outdoor storage for at least another 25 years, there is a potential for cylinder wall failures which may lead to atmospheric releases of UF_6. ANSI N14.1 specifies that wall thicknesses of nominally 5/16" (8 mm) thick cylinders do not fall below 1/4" (6.4 mm).

Early monitoring involved visual inspection, documentation of corrosion damage, evaluation of potential monitoring techniques and establishing a corrosion coupon monitoring program.[1-3] Cylinders were initially coated with a zinc chromate primer and an enamel topcoat, but most of these coatings have weathered away since they were not designed for long term outdoor storage. Many of these cylinders are now typically covered with thick corrosion scale, large pieces of which have spalled off the sides and bottoms. Surfaces are covered with deep pits and areas have developed a 'rock candy' appearance. Spot measurements using ultrasonic thickness gauges have shown uniform wall thinning of the order of 20 mils (0.5 mm) and pits up to 100 mils (2.5 mm) deep, indicating that a significant number of cylinders may have areas which have thinned down below ANSI N14.1 limits.

It is well known that the extent of corrosive attack on structures exposed to the atmosphere varies with the micro-climate around the structure as well as with the nature of exposure of individual areas of the structure.[4-18] Factors influencing corrosion such as time-of-wetness and the constituents of the immediate environment are in turn affected by the nature of the exposed surface, drainage, and humidity conditions. A wide range of corrosion behavior may therefore be expected. A wide variety of cylinder damage has been observed, but the distribution of damage and number of cylinders in need of corrective action of some sort is unknown at this time. In 1992, a detailed experimental program was initiated to characterize and monitor the atmospheric corrosion damage of the cylinders and provide guidelines for corrective actions.

EXPERIMENTAL PROCEDURES

Most of the UF_6 cylinders are stored in 2 unprotected yards, designated as E-yard and K-yard. The UF_6 cylinders are stacked in two-high rows, with the bottom row cylinders supported on contoured wooden saddles and the top row cylinders resting in the valleys between bottom row cylinders. The wooden saddles are designed to keep the bottoms of cylinders 4" (100 mm) off the ground. Top or bottom row cylinders are typically spaced a few inches apart within a row (although they are often in contact) and cylinder rows are typically a few feet apart allowing access for inspection and maintenance. The surface of E-yard is concrete and K-yard is part concrete, part compacted gravel. The concrete surface of E-yard is relatively even and intact, with good drainage of rain water, whereas the concrete in K-yard is buckled and broken in several areas, leading to uneven drainage and water pooling. In some of these areas, cylinders have sunk into ground contact. The compacted gravel area is relatively well drained. Figure 1 shows a typical stacking arrangement of cylinders on the concrete pad in K-yard. Figure 2 shows examples of heavy corrosion scale and pitted surfaces on cylinders.

Based on these cylinder yard conditions, three locations were chosen for primary monitoring - one in E-yard and one each in the broken concrete (K-south) and compacted gravel (K-north) areas of K-yard. A top row and underlying bottom row cylinder were instrumented at each location. The sensors were pre-mounted on 3" (75 mm) wide, 25 mils (0.625 mm) thick stainless steel bands using a strain gauge-mounting epoxy mixed with copper powder to improve the thermal conductivity

DISCLAIMER

DISCLAIMER

Portions of this document may be illegible in electronic image products. Images are produced from the best available original document.

between the sensor and the mounting surface. The bands were cinched tightly around the cylinders. A coating of a silicone-based adhesive was applied over the encapsulated surfaces, lead wires and soldered junctions taking care to keep the active sensor elements clear. Each band had two sets of sensors, located on the top and bottom surfaces of the cylinder to which the band was attached. Each of the 3 primary cylinder locations therefore had 4 sensor sets, distributed 2 each on a top row and a bottom row cylinder. This arrangement allowed corrosion monitoring as functions of cylinder position as well as location on the cylinder surface. Separate bands, mounted adjacent to each other, were used for the time-of-wetness and corrosion probe sensor sets.

Each time-of-wetness sensor was mounted with a thermocouple adjacent to it. The time-of-wetness sensor is a resistance type copper grid. Sereda-type copper-gold bimetallic sensors[10,11] were also attached to the bands, but have not been used since it was felt that the larger surface area of the copper resistance-type sensors would provide a greater degree of robustness. Each of the three primary locations also has a weatherhead located at ground level. The weatherheads are equipped with a rain gauge, a relative humidity sensor and a thermocouple for ambient temperature measurements. Data from the sensors/gauges are downloaded every 10 minutes into a datalogger. A total of 12 time-of-wetness sensors have been deployed among the 3 cylinder locations described above.

The corrosion probes used were of the electrical resistance type. The 8 mils (0.2 mm) thick plain carbon steel probe element was mounted on a fiberglass backing with further fiberglass encapsulation of the reference element. The carbon steel is a good approximation to the A-285 and A-516 steels used in UF_6 cylinder construction. The approximate overall dimensions of the probe are 3" (75 mm) long x 1" (25 mm) wide x 1/16" (1.6 mm) thick. The electrical resistance of the probes was monitored using a dial-type portable electrical resistance monitor. Good correlation has been found in field studies comparing atmospheric corrosion of electrical resistance corrosion probes and conventional weight loss coupons.[12] Initial probe readings were recorded at the time of deployment, after which the probes were typically monitored at one or two week intervals.

A total of 56 corrosion probes have been deployed, 12 of which were in conjunction with time-of-wetness sensors, as described above. The remaining probes have been distributed in several areas including on corrosion coupon racks, in the laboratory area and at strategic cylinder locations and are oriented facing the sky or ground and in a sheltered or open position.

Sets of 4" x 6" (100 mm x 150 mm) coupons of A285, A516 and A36 steels have been deployed at orientations of 0° and 30° to the horizon on south-facing coupon racks in E-yard and K-yard ('ASTM G50 coupons'). Scheduled retrievals of 4 replicates are at 1-, 2-, 4-, 8- and 16- years intervals following ASTM G50 guidelines.[13] After retrieval, mass losses and corrosion rates are measured after dissolving the corrosion products in a solution of 0.5 g/l sodium lauryl sulfate, 100 ml/l concentrated hydrochloric acid and 125 g/l sodium hypophosphite. Data from 1- and 2- years exposures have been collected to date.

In addition to coupon rack exposures, sets of A516 steel coupons have also been mounted directly on cylinder surfaces ('cylinder coupons') to monitor differences in local corrosivities. In order to restrict corrosion to only one exposed face, the A516 coupons were attached to mild steel coupons with double-sided adhesive tape.[14] The mild steel side of the combination was then attached to cylinder surfaces using small neodymium-iron-boron magnets, leaving the A516 side exposed. After exposure, the two pieces are separated and corrosion rates estimated after removing the corrosion products from the single exposed face of each coupon. Sets of coupons (3 replicates) have been deployed for 1-, 2-, 4-, 8-, and 16-years exposures on the K-yard coupon rack and on 5 groups of cylinders, including the 3 cylinder groups with time-of-wetness sensors and corrosion probes. In each cylinder group, the coupons have been placed on top of the top row cylinder and on the top and bottom of the bottom row cylinder (no coupons were attached to the bottom of the top row cylinders). To date, data from 1-year exposures have been collected. Additional coupons have been recently exposed in ground contact near the cylinder locations, to estimate effects of direct cylinder contact with the ground.

Figure 3 shows a cylinder with stainless steel straps with attached time-of-wetness sensors, thermocouples and corrosion probes. A few of the A516 steel cylinder coupons are also visible in the photograph.

The cylinders are visually inspected routinely, and supplemental information is obtained from these inspections. In addition, a parallel inspection program has been measuring cylinder wall thicknesses using ultrasonic thickness gauges and an automated ultrasonic scanning system capable of traversing the circumference of a cylinder was recently obtained. These data, not presented here, provide a measure of actual metal loss around the cylinders due to uniform and pitting corrosion.

RESULTS AND DISCUSSION

A major objective of the program was to identify any differences in corrosivity as a function of cylinder location and stacking position. The three primary cylinder locations, representing varying water drainage and storage conditions, were chosen with this in mind. There are three main sources of data: time-of-wetness, corrosion probes and corrosion coupons and the results are presented separately below. Sensor/coupon locations are identified by stacking position and location on the cylinder. For example, TR, T refers to a position on top of a top row cylinder, BR, T refers to the top of a bottom row cylinder etc.

Time-of-Wetness: Trends.

Time-of-wetness data and total monthly rainfall (average from rain gauges in E- and K-yards) are summarized in Table 1. The times-of-wetness are presented as the fraction of time the sensor was 'wet'. The onset of wetting was arbitrarily defined as an output of 200 mv (the sensors have a full scale reading of 2500 mv). Two main observations can be made from Table 1:

1. Sensors on top of cylinders tend to stay wetter than sensors mounted on cylinder bottoms, irrespective of yard or stacking position. Significant wetness on cylinder bottoms is observed mainly during months of the heaviest rainfall (March 1993, January - March 1994) although there are months when the extent of BR, B wetting does not correlate with the amount of rain(February 1993, December 1993, April 1994, June 1994).

2. In general, there is no significant difference in wetness times between the well-drained concrete surface in E yard and the poorly drained broken concrete area in K-yard. However, there are potential trends in that the TR, T position at K-north appears consistently drier than the other locations as does the BR, B sensor in the broken concrete area at K-south, which one may have expected to be wetter because of poor drainage. There is no apparent physical reason for these observations and the explanation may lie in a lower sensitivities of these sensors compared to the others. Although the sensors were conditioned prior to deployment according to ASTM recommendations for Au/Cu sensors,[11] no calibration tests have been performed in order to establish differences in response sensitivities. These are currently underway.

Time-of-Wetness: Wetting Behavior and Orientation Effects.

Figures 4(a) and 4(b) show responses from TR, T and BR, B time-of-wetness sensors along with rainfall data collected during two time periods in April, 1994 at the K-south location. The results are typical of all three locations. As can be seen, there are several instances when the TR, T sensor triggered a positive response over time periods with no rainfall. These include the early morning hours of April 2, 4, 5, 10 and 12. In each of these instances, the remaining 3 sensors at the installation did not trigger. The positive responses are apparently due to dew formation on the sky-facing top surfaces during the early morning hours. Similar observations have been commonly reported in the past,[9,10,17,18] as has the fact that condensation can be the major contributor to total wetness times[9,17] and often triggers a lower sensor response than rain,[19] as observed here. The top surfaces undergo greater cooling due to radiative heat loss than bottom facing surfaces, and surface temperatures are more likely to go below the dew point, leading to condensation. This is supported by thermocouple data from the cylinder surfaces. Data from the same time period as Figure 4(a) from TR, T and BR, B surfaces at K-south are shown in Figure 5. It is clear that the TR, T surface undergoes much greater temperature swings during a 24-hour period than the BR, B surface, which stays fairly close to ambient temperatures. The large fluctuations are due to radiative heating and cooling, the effects of which are magnified by an empty head space in the UF_6 cylinders. Temperature variations of bottom surfaces are moderated by the large heat mass of UF_6 in contact with these surfaces. Over the course of a day, both the highest and lowest temperatures are measured on cylinder tops, which evidently cool down below the dewpoint at night, causing condensation. Note that on April 3, there was no apparent dew formation (Figure 4(a)). This can be related to significantly less cooling of the cylinder surface (Figure 5), probably due to cloud cover prior to rain later in the day (Figure 4(a)).

Figures 4(a) and 4(b) also provide further details on wetting behavior. The rain events on April 4 and April 6 were not enough to trigger the BR, B sensor: the sensor triggered only over the next rain period on April 7. It triggered again on the next rain on April 11, but this time the sensor stayed 'on' for 3 days even though no rainfall was measured and the TR, T sensor switched off. These results suggest that cylinder bottoms stay dry even during rain periods - until a critical frequency and/or amount of rain is exceeded. Once the bottoms are wet, they apparently stay wet longer than top surfaces, perhaps related to the general isolation of the areas and frequency of rain and cloudiness during the period of drying.

This view is supported by the data in Figures 6(a) and 6(b), which show rainfall data as well as periods when TR, T and BR, B time-of-wetness sensors were 'on' during December 1993 and January 1994. (Some of the precipitation occurred in the form of ice or snow. However, sunshine and/or daytime temperatures typically melted the solid precipitation on contact or within a few hours. There was only one instance, towards the end of January, when solid precipitation was present for a period greater than 24 hours.) The time intervals shown, 27 days in Figure 6(a) and 34 days in Figure 6(b), experienced roughly equal amounts of total rain. In the period shown in Figure 6(a), the BR, B sensor was triggered only over 2 time periods representing 6.8% of the time interval, compared to a 39.6% 'on' time for the TR, T sensor. In contrast, for the period shown in Figure 6(b), both TR, T and BR, B sensors stayed 'on' for 38.3% of the time. Note that the response of the TR, T sensor was very similar over both time periods. The difference between Figures 6(a) and 6(b) is that in the first case, rain events were relatively heavy but few, typically occurring every 5 days. During the second time period, rain was less heavy but at a higher frequency. Note that towards the end of January with several rain events over the last few days, the BR, B sensor stayed 'on' for a period of over a week. This is similar to the observation made earlier with respect to Figure 4(b). Note also that in both Figures 6(a) and 6(b), the initial triggering of the BR, B sensor was always significantly after that of the TR, T sensor.

It may be argued that bottom surfaces may be expected to stay damp longer due to lower evaporation and closer proximity to the ground, especially under wet ground conditions in poorly drained areas. However, these data support the conclusion that cylinder bottoms stay drier than cylinder tops because a significant amount of frequent precipitation is needed for the wetness to reach and cover these areas. Experience with similar instrumentation of UF_6 cylinders at a facility in Paducah, KY has shown that cylinder bottoms there tend to stay significantly wetter, with visible near-constant dampness.[22] This may be a result of significantly different ground conditions due to local rainfall, water tables, humidity conditions etc. Not surprisingly, corrosion probes at the Paducah site also show higher corrosion rates along cylinder bottoms, contrary to the observations at Oak Ridge as described below.

One relationship which could not be established conclusively was that between relative humidity and time-of-wetness. The relative humidity sensors typically broke down after 2-3 months, and practical considerations prevented immediate replacement of the sensors. In general, there was a fairly good correlation between relative humidity and time-of-wetness readings. It appeared that the time-of-wetness sensors showed a positive reading only when relative humidity levels were over 50%, and had readings over 200 mv (the 'on' threshold) only at relative humidity readings greater than 70-80%. This agrees well with observations in the literature.[5,9,10,15,17,19]

Corrosion Probes: Trends and Orientation Effects.

The corrosion probes were installed between February and December 1993, mainly between late March and early July. Results from the various locations have generally been similar. No differences have been observed between K-yard or E-yard, or between locations within a yard. All differences in data appear to be directly related to the orientation of the probes. Figure 7 shows typical data, from the K-north location. Corrosion rates are measured as the slopes of the metal loss versus time plots. Several trends were noted:

1. Probes exhibit an incubation period before the probe dial readings begin to increase, i.e., before measurable corrosion occurs. The incubation period is significantly longer on probes attached to bottom surfaces of cylinders.
2. Probes trends can be grouped based on whether they are mounted on top or bottom surfaces of cylinders. These trends are irrespective of whether the cylinder is in a top or bottom row.
3. Significantly higher corrosion rates (measured after incubation) are observed from probes on cylinder tops than from probes on cylinder bottoms. However, these corrosion rates appear to moderate in some cases at later stages (e.g., probe #3).

Figure 8(a) shows data from a set of probes attached to the corrosion coupon rack in K-yard. These probes were attached in orientations shown in Figure 8(b), meant to replicate probes on cylinders. The trends seen in Figure 8(a) are very similar to those seen in Figure 7. Top-facing open probes (#34 and #37) have shorter incubations and corrode faster, at least initially. The moderation in corrosion rates (change in slope) typically occurred after about 200 days of exposure for most top-facing probes (see also Figure 7).

Figure 9 summarizes the corrosion probes data from several locations, including the three primary locations, the coupon rack and several other installations in K-yard. The data are presented as corrosion rates calculated from plots as in Figures 7 and 8(a) which can often be broken up into several linear segments having different slopes - i.e., different corrosion rates. Data for '150 days' represent corrosion rates existing after 150 days exposure, which typically correspond to post-incubation for top facing probes but is often still within incubation for down facing probes. Data for '>300 days' for all probes represent the trend being observed in the last 100 days of data gathering. Total exposure periods range from approximately 300 to 500 days. Figure 9 shows that in most cases, corrosion rates of top-facing probes decreased significantly after initial incubation and a period of relatively high corrosion rate. The '>300 days' corrosion rates are often similar to those measured from down-facing probes, which typically show minimal corrosion for relatively long time periods before exhibiting a slight upward trend in corrosion rates. The data summarized in Figure 9 show no obvious effects of poor or good drainage or of yard-to-yard differences.

Higher initial corrosion rates observed on top mounted probes are supported by higher wetness times measured in these areas. These results are probably not influenced by the cylinders or their contents, since similar orientation effects were observed from probes on coupon racks and in between cylinders. As discussed above, preferential dew formation on sky-facing surfaces at night appears to be the most reasonable explanation. Condensed moisture has been associated with higher corrosion rates compared to precipitated moisture due to a lack of washing action.[4,21] Further, aided by greater exposure to rain, the upper surfaces would stay wetter longer, leading to higher corrosion rates.

Corrosion Probes: Effects of Shelter.

The long incubation periods and low corrosion rates associated with the down-facing probes (which include bottom-mounted probes on cylinders) are also seen in top-facing probes which are sheltered (Figure 8(a), probes #36 and #40). These undergo less corrosion than open, down-facing probes (probes #38 and #39). (See also data for K-yard rack probes in Figure 9.) These results imply that surfaces protected from wetting undergo less corrosion, at least to the point that the onset of corrosion is delayed significantly. Probes distributed in spaces between top row cylinders in K-yard in the orientation shown in Figure 8(b) showed results very similar to that observed in Figure 8(a).

The data show that corrosion rates of open and protected probes eventually approach similar values, and the long incubation periods of protected probes appear to be directly related to delayed wetting of such surfaces. Once the corrosion product forms, corrosion proceeds at relatively high rates (Figures 7 and 8), even though neighboring time-of-wetness sensors (where present) continue to show relative dryness in these locations. Apparently, once a corrosion product forms, the corrosion process is more easily maintained, perhaps due to hygroscopic properties of the rust layer. In other words, the rust layer could be 'wet' while an adjoining time-of-wetness sensor could be 'dry'. Apart from implying that any beneficial effects of shelter/protection is only felt as long as corrosion is not initiated, time-of-wetness measurements would tend to underestimate relative corrosion in such cases. Note however that the slopes of most of the open top-facing probes eventually decrease, leading to an overall drop in corrosion rates (Figure 9). This suggests that a protective corrosion product does eventually form on the probes. This would also suggest that protected probes may also eventually show a second transition (change in slope) much like the open, top-facing probes, thus reflecting advantages of sheltered exposure. Effects of hygroscopic and other properties of rust layers on corrosion have been reported in the literature.[4,6,7,9,12,14] In addition, as discussed below, beneficial effects of sheltering often exist only over relatively short time periods,[8,12,15] as seen to date in this study.

Corrosion Probes: Corrosion Product Development.

Typical visual observations of probes showed that, after about 150 days exposure, top-facing probes were completely covered with a flaky rust layer whereas bottom-facing probes still had large uncorroded areas visible. The extended incubation and negligible initial corrosion rates observed in bottom-facing probes can be related to a delay in the start of the corrosion process. Appearance of significant corrosion products on bottom-facing probes were seen after 300-500 days exposure, associated with significant increases in corrosion rates as shown in Figure 9.

In order to more closely relate probe response to changes in its appearance and weather, 3 probes were installed in the loading dock area of the laboratory building: one horizontal and facing up (probe #54), the second horizontal and facing down (probe #55) and the third facing up but sloping downward at an angle of 45° (probe #56), to allow water to drain off. The probes were monitored on at least a daily basis for the first few weeks of exposure. Again, the bottom facing probe showed the longest incubation time, but achieved a corrosion rate similar to the top facing probe once corrosion started. Visual inspections showed that probe #54 quickly developed a rust layer on its surface (completely rust covered within 7 days) whereas probe #55 had large rust-free areas even after 40 days of exposure. During rain events, probes #54 and 56 were quickly wetted whereas probe #55 stayed mostly dry, with occasional wetting from wicking action of water beads forming on the edges of the covering surface.

Figure 10 shows data from probe #54 covering a few periods of precipitation. Corrosion is clearly associated with periods of wetness, but appears to increase after the end of the rain - as the water bead evaporates. Such discrete jumps in metal loss were not seen in the other two probes and agrees with the model of atmospheric corrosion of iron being dominated by corrosion during the drying stage of a moisture deposition/evaporation cycle.[20] Figure 10 also presents ambient temperature data showing that the corrosion process does not seem to be influenced by the temperature, at least in the range encountered.

Corrosion Probes: Other Issues.

Sets of probes were installed in late-May and late-October, yet show similar trends. This suggests that any seasonal effects on corrosion are minimal, although a careful analysis shows that they cannot be discounted. Metal loss versus time data for all the probes were examined, and 32 probes were identified which showed a decrease in the slope (corrosion rate) in the post-incubation region, as can be seen in Figure 7 for probe #3 after about 210 days and probe #4 after 400 days or in Figure 8(a) for probe #34 after 150 days. A tabulation of all the data showed that in 16 of the 32 cases, the decrease in slope was initiated in the months of November-January, suggesting a wintertime slowdown in corrosion rates. However, 14 of these 16 'slowdowns' occurred starting 150-230 days from initial exposure and 15 of the 16 probes were top-facing open probes, suggesting that the 'slowdown' is more related to the time-dependant buildup of certain type(s) of corrosion products. This issue is currently unresolved. It may also be noted that many probes showed an increase in corrosion rate after some period of 'slowdown', typically of the order of 60 - 90 days (see Figure 8(a)).

Although the general behavior of top and bottom facing probes as two separate groups is similar, there are differences in individual probe behavior which are unexplained. An example is probe #1 in Figure 7. The lack of a transition to a lower corrosion rate is unusual, and cannot be explained at present. Similarly, in Figure 8(a), top-facing open probes #34 and #37 appear to diverge significantly in behavior after showing similar responses for the first 150 days of exposure. In these set of probes, only probe #34 among the 'open' installations appears to show an interim transition to a lower corrosion rate. Further, the subsequent increase in corrosion rate in probe #34 after 320 days is also unexplained. Some of these discrepancies must surely be related to seasonal changes and chemistry and morphology of the corrosion products developed on the probes. Recently, three of the probes (including probe #1 in Figure 7) reached the end of useful data collection life and 'topped out', having undergone 4 mils (0.1 mm) of metal loss. These probes will be destructively analyzed and it is hoped that corrosion product analysis and continuing data collection will help resolve some of the questions regarding probe behavior.

Corrosion Coupons: Trends and Orientation Effects.

Data from 1- and 2-year exposures of ASTM G50 coupons are shown in Figure 11. Higher corrosion rates were observed in the first year of exposure, as is typically observed in atmospheric exposures. In the second year, the corrosion rates drop off to 0.5 - 0.7 mpy (12.5 - 17.5 μm/y), which is what may be expected in the rural atmosphere around the non-operating plant at Oak Ridge. One interesting trend which may be developing in Figure 11 is the higher corrosion rates measured in E-yard. The rates are at least 50% higher in the first year and about 30% higher in the second year. It is unclear if the differences will narrow over the next set of retrievals. This trend is not supported by any of the other monitoring techniques. Physically, E-yard is located close to a river and often tends to be fog-covered when K-yard is not. However, any excess wetness is not reflected in the time-of-wetness data. It is possible that careful analysis of the data after calibrating the time-of-wetness sensors for relative sensitivities may establish differences.

Figure 12 shows data from 1-year exposures of the A516 steel cylinder coupons. The corrosion rates measured from these single-sided coupons are significantly higher than those from the 2-sided ASTM G50 coupons. Part of the reason is undoubtedly due to the sheltering of bottom surfaces in the latter case. There may also have been contributions from undercutting around the taped edges of the cylinder coupons. This was clear in some of the coupons in which the tape had delaminated in places, and may also contribute to the larger scatter seen in these data compared to Figure 11. The data in Figure 12 also indicate higher corrosion rates among the cylinder coupons compared to those on the coupon rack, with very high corrosion rates in the poorly drained K-south location and the highest corrosion rates among coupons on cylinder tops. However, these differences may narrow over the next sets of retrievals and any conclusions drawn from this first set of data would be premature.

Corrosion Coupons: Pitting Behavior.

Top facing coupons were also significantly more heavily pitted than bottom facing coupons, which may contribute to their generally higher mass losses. Figure 13 shows the results of pit depth measurements on the 1-year cylinder coupons after the corrosion product had been rinsed off. Twenty of the deepest appearing pits were measured using an optical microscope with a calibrated focussing knob, and, of these, the fifteen highest values were averaged for each data point. There is significant scatter in the data, but at each location pit depths on bottom row, bottom coupons are consistently lower than on the sky-facing coupons. Again it is too early to say if pitting on bottom facing coupons is fundamentally less or is merely delayed due to sheltering effects. Examination of two-sided ASTM G50 coupons exposed on the coupon rack for 2 years showed pits on both sides of the coupons, with no clear indication if the pits were deeper on any one side. This suggests that with time, pitting on skyward faces becomes as severe as on sheltered surfaces. Unfortunately, none of the 1-year ASTM coupons were available for comparison in order to verify any aging effects. It is generally observed that pitting corrosion is deeper and denser on rain-protected surfaces,[4,16] - reverse of the 1-year cylinder coupons results in the present study. It will be interesting to see how the pits develop in succeeding years.

General Discussion.

There is, in general, excellent correlation between the time-of-wetness and corrosion probe data. However, there is one piece of data at Oak Ridge which contradicts the corrosion probes and time-of-wetness data as well as the preliminary data from cylinder coupons. Visual observations and ultrasonic thickness measurements of cylinders in K-yard have shown that many cylinders have experienced greater thinning near the bottoms, ostensibly due to higher corrosion rates. The greater thinning is in terms of both thinner cylinder walls (average uniform thickness) and deeper pits. This is not supported by results from any of the corrosion monitoring techniques. The preferential bottom thinning may be related to the effects of previous storage. The cylinders had been stored for a number of years on an asphalt surface which had badly deteriorated under the cylinders' weight, so that a large number of the cylinders were in ground contact for a number of years. Unfortunately, no tracking records exist to correlate observations with cylinders history. Cylinders in E-yard have been constantly maintained at that location and visually appear to be less corroded than those in K-yard. However, ultrasonic measurements are yet to be done on these cylinders in order to confirm or refute preferential bottom thinning. Thinner bottoms on K-yard cylinders cannot be reconciled with the currently available data, and can only be attributed to previous poor storage conditions.

Seasonal effects, as reflected by different corrosion rates for samples initially exposed at different times of year,[4,7,17] were not observed in the corrosion probes data except for the possible trends discussed earlier. As in the examples shown in Figure 8, corrosion-time curves appear to be primarily influenced by the probe orientation; curve shapes and lengths of individual segments appear to be independent of the time of initial exposure. It may be noted that seasonal differences reported in the literature often disappear at long exposures.[7] Seasonal effects, usually reflected as higher corrosion rates for winter-commenced exposures, are usually attributed to higher SO_2 levels in winter.[4,7,17] Such situations may only be important in relatively industrial locations, unlike the Oak Ridge K-25 Site.

The literature shows contradictory reports on the effects of skyward (open) or sheltered surfaces on wetting response[6,9,17,18] and atmospheric corrosion.[7,8,12,14-16] Times-of-wetness on skyward surfaces have been reported to be sometimes more,[18] sometimes less[9,17] and sometimes both more or less[6] than on groundward surfaces. In many cases, sheltered surfaces experienced lower corrosion rates as they were protected from the elements[8,12,14] (as apparently in the present study), but in other cases, sheltering only served to create a more hostile 'micro-environment' which increased the corrosion rates. In situations where there was a tendency for corrosive species to deposit, as perhaps in industrial environments, open surfaces benefitted from a washing action of rain leading to lower corrosion rates.[7] However, in other examples, no clear trends were observed as corrosion rates of open specimens were sometimes higher and sometimes lower than that of sheltered specimens for multiple exposures at the same location.[15,16] In most cases, results have been explained on the basis of specific environmental conditions existing at each test site or during the test schedule, underlining the importance of accurately characterizing the immediate environment.

Many of the orientation effects and preliminary trends observed in the present results and in the literature appear to be strictly valid only over relatively short exposure times, typically less than 2 years. Literature data showing strong effects either have no long term data or show narrowing differences as exposure times increase. A summary of some literature observations relating to time-of-wetness and atmospheric corrosion is presented in Table 2. In 5 of the 8 cases shown, initial differences in corrosion behavior (as a function of season, orientation etc.) evened out or reversed over longer time periods. Most of the authors reported and discussed data over relatively short time frames (3 of the 8 studies covered only 12 months). Although this time frame may be suitable for accelerated or quick response tests (e.g., corrosion probes), the corrosion characteristics of traditional coupon-type tests probably have not developed steady-state features. For example results from 12 month exposures of corrosion coupons[6] could not be correlated to factors like time-of-wetness or atmospheric pollution. Comparisons with and inferences drawn from the literature should therefore be done with care, and most experimental results are probably best explained by local criteria rather than a set of universally applicable guidelines, except in a very generalized manner.

SUMMARY AND CONCLUSIONS

An atmospheric corrosion monitoring program using time-of-wetness sensors, corrosion probes and corrosion coupons has been ongoing at the U.S. Department of Energy's Oak Ridge K-25 Site repository of UF_6 cylinders. Major results and observations to date may be summarized as follows.

1. Results from the time-of-wetness sensors and corrosion probes are in good agreement but do not completely agree with early data from the corrosion coupons.

2. Data from the time-of-wetness sensors and corrosion probes show no significant effect of cylinder yard, row or stacking position. However, some time-of-wetness sensors read consistently higher or lower than others for no clear reason, and this may be due to differences in sensitivities between the sensors. Early data from the corrosion coupons show possible yard and stacking differences, but it is too soon to form any conclusions.

3. Areas on top of cylinders tend to stay wetter than cylinder bottoms. This appears to be related to more dew formation on top surfaces as well as due to the inaccessibility of bottom areas to rain except during heavy or frequent precipitation.

4. Metal loss versus time curves from all corrosion probes show similar shapes. All probes exhibit an incubation period and a period of increased metal loss, followed by a moderation in corrosion rates in many cases, especially amongst top-facing probes.

5. The length of the incubation period is related to the first appearance of corrosion products and is significantly shorter on top-facing, open probes. Observations of the corroding surface support the model of atmospheric corrosion being dominant during the drying stages of an initially wet surface, at least during the early stages of corrosion product development.

6. The effects of sheltering are manifested in corrosion rates that are, at least initially, significantly higher on cylinder tops (top-facing, open probes) than bottoms (protected surfaces), an observation that is well supported by time-of-wetness data. Protection appears to delay the onset of corrosion by keeping surfaces dry, and corrosion rates on such surfaces increase once a corrosion product forms. However, there are not enough results to establish any final long-term differences in corrosion rates between the two types of exposures.

7. Corrosion probe data show no significant seasonal effects, although such effects could not be ruled out.

8. The probes and time-of-wetness data do not agree with ultrasonic measurements which have shown greater thinning and pitting on some cylinder bottoms compared to tops. This observation may be related to damage caused by prior storage in which the cylinder bottoms may have been in ground contact, leading to severe corrosion.

9. Apart from possible yard-to-yard and cylinder position differences in corrosion rates, early data from corrosion coupons also indicate a higher degree of pittting on cylinder tops. However, the data are very limited and longer exposure times are required for trends to be confirmed.

The atmospheric corrosion monitoring program at the Oak Ridge K-25 Site is relatively young and many of the observed trends are still developing. Comparison with literature data shows support for the various observations made during this study. However, not all observations are in complete agreement and significantly different trends have also been reported from a facility in Paducah, KY which uses the same monitoring techniques. This emphasizes the need for careful analysis of data based more on local conditions than on universal guidelines, except in a generalized manner.

ACKNOWLEDGEMENTS

This work was funded as part of the Department of Energy's UF_6 Cylinders Project at Martin Marietta Energy Systems, Valerie Newman, Program Manager. The ultrasonic thickness data were provided by Halen Philpot. Hardware setup and data collection were done by Ron Adamski, Jeff Broders, Alvin Ellis, David Freels, Glenn Harris, Don Kelley and Bonnie Phillips. Significant input and guidance on the UF_6 Cylinders Project were provided by Curtis Barlow, Helen Henson and Ken Ziehlke.

REFERENCES

1. H. M. Henson, J. L. Frazier, C. R. Barlow and K. T. Ziehlke, "Monitoring of Corrosion in ORGDP Cylinder Yards", in *Uranium Hexafluoride - Safe Handling, Processing and Transporting Conference, Oak Ridge, TN, May 24-26,1988*, W. D. Strunk and S. G. Thornton, eds., CONF-880558-2, Oak Ridge Gaseous Diffusion Plant, 1988, pp. 103-110.
2. H. M. Henson, V. S. Newman and J. L. Frazier, "An Update on Corrosion Monitoring in Cylinder Yards", in *Second International Conference on Uranium Hexafluoride Handling, Oak Ridge, TN, October 29-31, 1991*, CONF-9110117, Oak Ridge National Laboratory, 1991, pp. 131-134.
3. UF_6 Containment and Storage Committee, *Containment and Storage of Uranium Hexafluoride at U.S. Department of Energy Uranium Enrichment Plants*, K/ETO-99, Oak Ridge K-25 Site, Oak Ridge, TN, June 1992.
4. K. Barton, *Protection Against Atmospheric Corrosion*, John Wiley and Sins, New York, 1972.
5. P. J. Sereda, "Weather Factors affecting Corrosion of Metals", in *Corrosion in Natural Environments*, ASTM STP 558, American Society for Testing and Materials, 1974, pp. 7-22.
6. H. Guttman and P. J. Sereda, "Measurement of Atmospheric Factors affecting the Corrosion of Metals", in *Metal Corrosion in the Atmosphere*, ASTM STP 435, American Society for Testing and Materials, 1968, pp. 326-359.
7. C. P. Larrabee, "Corrosion Resistance of High-Strength Low-Alloy Steels as Influenced by Composition and Environment", *Corrosion*, v. 9, 1953, pp. 259-271.
8. J. P. Carter, P. J. Linstrom, D. R. Flinn and S. D. Cramer, "The Effects of Sheltering and Orientation on the Atmospheric Corrosion of Structural Metals", *Materials Performance*, July 1987, pp. 25-32.
9. H. Guttman, "Atmospheric and Weather Factors in Corrosion Testing", in *Atmospheric Corrosion*, W.H. Ailor, ed., John Wiley and Sons, New York, 1980, pp. 51-68.
10. P. J. Sereda, S. G. Croll and H. F. Slade, "Measurement of the Time-of-Wetness by Moisture Sensors and Their Calibration", in *Atmospheric Corrosion of Metals*, ASTM STP 767, S. W. Dean Jr., and E. C. Rhea, Eds., American Society for Testing and Materials, 1982, pp. 267-285.
11. *Standard Practice for Measurement of Time-of-Wetness on Surfaces Exposed to Wetting Conditions as in Atmospheric Corrosion Testing*, ASTM Standard G 84-89, American Society for Testing and Materials, 1989.
12. M. McKenzie and P. R. Vassie, "Use of Weight Loss Coupons and Electrical Resistance Probes in Atmospheric Corrosion Tests", *Br. Corros. J.*, v. 20, 1985, pp. 117-124.
13. *Practice for Conducting Atmospheric Corrosion Tests on Metals*, ASTM Standard G 50, American Society for Testing and Materials, 1989.
14. R. A. Legault and V. P. Pearson, "Kinetics of Atmospheric Corrosion of Galvanized Steel", in *Atmospheric Factors Affecting the Corrosion of Engineering Metals*, ASTM STP 646, S. K. Coburn, Ed., American Society for Testing and Materials, 1978, pp. 83-96.
15. S. Feliu and M. Morcillo, "Atmospheric Corrosion Testing in Spain", in *Atmospheric Corrosion*, W. H. Ailor, ed., John Wiley and Sons, New York, 1980, pp. 913-921.
16. M. McKenzie, "The Corrosion Performance of Weathering Steel in Highway Bridges", in *Atmospheric Corrosion*, W. H. Ailor, ed., John Wiley and Sons, New York, 1980, pp. 717-741.

17. H. Guttman, "Effects of Atmospheric Factors on the Corrosion of Rolled Zinc", in *Metal Corrosion in the Atmosphere*, ASTM STP 435, American Society for Testing and Materials, 1968, pp. 223-239.
18. P. R. Grossman, "Investigation of Atmospheric Exposure Factors that Determine Time-of-Wetness of Outdoor Structures", in *Atmospheric Factors Affecting the Corrosion of Engineering Metals*, ASTM STP 646, S. K. Coburn, Ed., American Society for Testing and Materials, Philadelphia, 1978, pp. 5-16.
19. J. J. Hechler, J. Boulanger, D. Noel, R. Dufresne and C. Pinon, "A Study of Large Sets of ASTM G84 Time-of-Wetness Sensors", in *Corrosion Testing and Evaluation: Silver Anniversary Volume*, ASTM STP 1000, R. Baboian and S. W. Dean, Eds., American Society for Testing and Materials, Philadelphia, 1990, pp. 260-278.
20. M. Stratmann, K. Bohnenkamp and T. Ramachandran, "The Influence of Copper on the Atmospheric Corrosion of Iron", *Corrosion Science*, v. 27, 1987, pp. 905-926.
21. R. S. Yamasaki, H. F. Slade and P. J. Sereda, "Determination of Time-of-Wetness due to Condensed Moisture", *Durability of Building Materials*, v. 1, 1983, pp. 353-361.
22. S. C. Blue, Martin Marietta Utility Services, Paducah, KY, Private Communication.

TABLE 1.
MONTHLY DATA FROM THE THREE TIME-OF-WETNESS SENSOR SETS. ONSET OF WETNESS IS DEFINED AS A SENSOR RESPONSE ABOVE 200 MV.

	E-Yard (% Time Wet)				K-Yard North (Gravel) (% Time Wet)				K-Yard South (Concrete) (% Time Wet)				Total Rain (")
	TR, T	TR, B	BR, T	BR, B	TR, T	TR, B	BR, T	BR, B	TR, T	TR, B	BR,T	BR,B	
Feb. 93	35.9	46.7	57.7	32.1	31.2	8.2	32.7	13.3	41.7	6.2	37.5	16.8	4.32
Mar. 93	50.9	62.8	55.3	45.5	41	13.2	38.3	37.1	57.9	10.2	52.8	28.4	7.0
Apr. 93	34.3	12.7	20.6	11.5	17.8	0	14	0	28.1	0	16.6	0	3.39
May 93	35.6	13	25.4	3.7	26.3	2	18.9	3	45	0	22.7	0	2.76
Jun. 93	-	0	17.1	0	10.9	0	10.9	0	-	0	16.4	0	1.5
Jul. 93	10.8	1.4	9.6	0.1	5	0	5.2	0	13.5	0	11.2	1.3	2.15
Aug. 93	23.4	0.1	20.1	0.1	9.7	0	9	0.1	25.8	0	16.4	0	3.48
Sep. 93	37.7	0.8	28.6	3.1	28.5	0	16.9	6.6	42.6	0	27.7	4.8	4.03
Oct. 93	46.2	8.1	34.2	17.1	37.8	3.3	22.9	20.35	48.1	3	35.8	16.5	1.92
Nov. 93	-	-	-	-	-	-	-	-	-	-	-	-	3.25
Dec. 93	40.2	5.9	28.3	6.7	27.4	3.4	28.5	6.9	33.9	3.3	37	4.2	6.68
Jan. 94	37.1	38.2	15.6	38.8	31.8	30	34.7	27.6	36.9	33.1	45.9	20.8	6.35
Feb. 94	34.5	21.1	17.8	38.8	28.7	26	29.7	38.2	34	23.8	32	27.6	9.6
Mar. 94	35	5	13	11	33	5	28	17	30	21	29	25	10.25
Apr. 94	25	1	5	13	20	1	14	16	24	1	14	12	8.82
May 94	27	0	13	0	16	0	10	3	26	0	15	0	2.77
Jun. 94	27	0	24	0	17	0	14	2	28	0	32	4	7.43
Jul. 94	36	0	27	6	24	0	19	3	34	0	35	9	5.93

TABLE 2.
LITERATURE OBSERVATIONS OF ATMOSPHERIC CORROSION BEHAVIOR AS RELATED TO LENGTH OF EXPOSURE.

Ref.	Material	Exposure Time	Summary of Observations
6	Cu, steel, Zn	1-12 months	Corrosion and atmospheric factors not correlated (e.g., site with highest corrosion rate of steel had relatively low time-of-wetness).
7	Steels	Up to 4 years	Corrosion-time curves influenced by season, but reach similar slopes (corrosion rate) at longest exposures.
8	Al, Cu, steel, Zn	3-12 months	Effects of shelter: Higher skyward corrosion rates, but differences narrow or reverse with time.
12	Steel	3-12 months	Effects of shelter/orientation: corrosion-time curves different but slopes (corrosion rate) similar after 3 months.
14	Galv. steel	1-5 years	Higher skyward mass losses throughout period.
15	Al, Cu, steel, Zn	Up to 4 years	Effects of shelter: some differences narrow or reverse by 4th year.
16	Cu, steel	1-5 years	Mixed effects of shelter; no reported time effects.
17	Zn	1-256 weeks	Short term seasonal variations in corrosion rates even out over time.

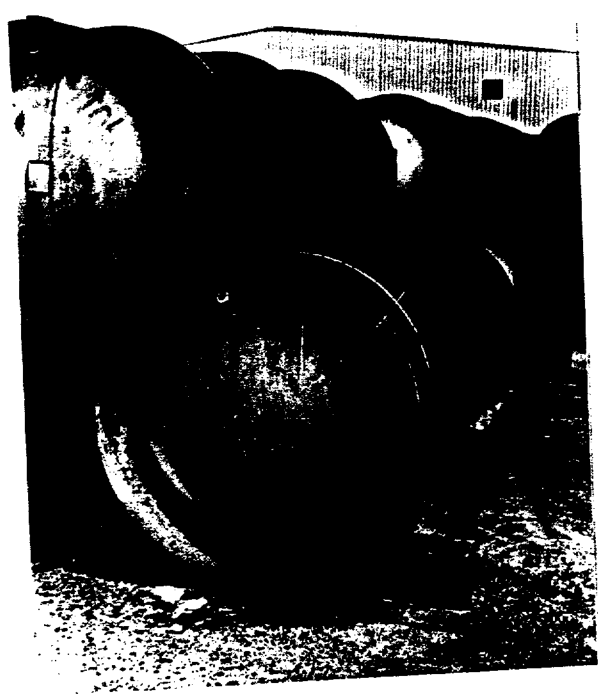

Figure 1. Typical stacking arrangement of UF_6 cylinders in the storage yards at the Oak Ridge K-25 Site. The location shown is the concrete surface in K-yard.

(a)

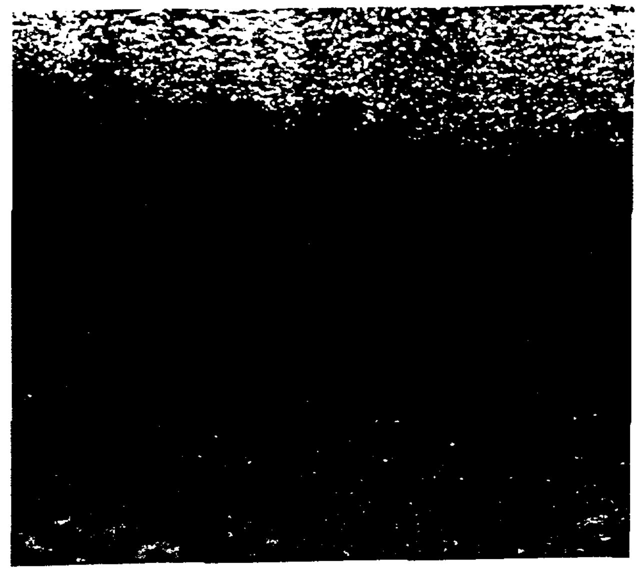

(b)

Figure 2. (a) and (b) Examples of heavy corrosion scale and pitted surfaces seen on UF_6 cylinders at the Oak Ridge K-25 Site.

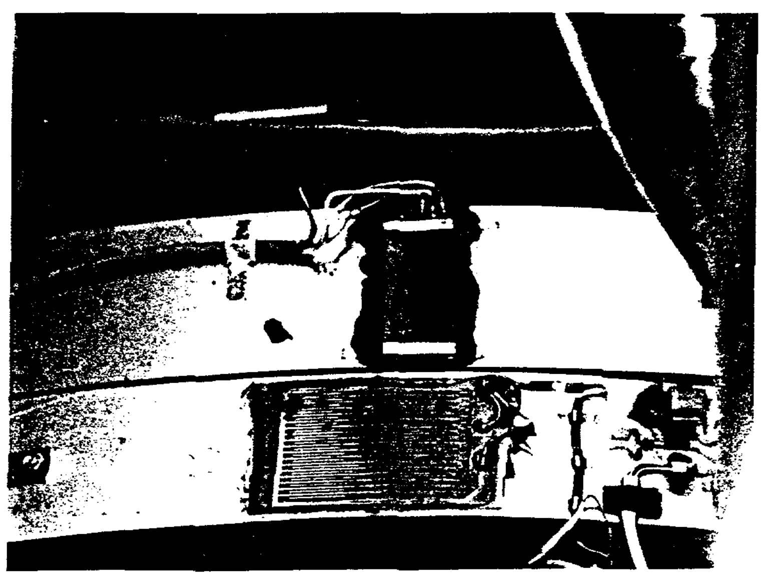

Figure 3. Cylinder instrumented with time-of-wetness sensors, thermocouples and corrosion probes on stainless steel bands and 1-sided A516 steel corrosion coupons attached to cylinder surfaces with magnets.

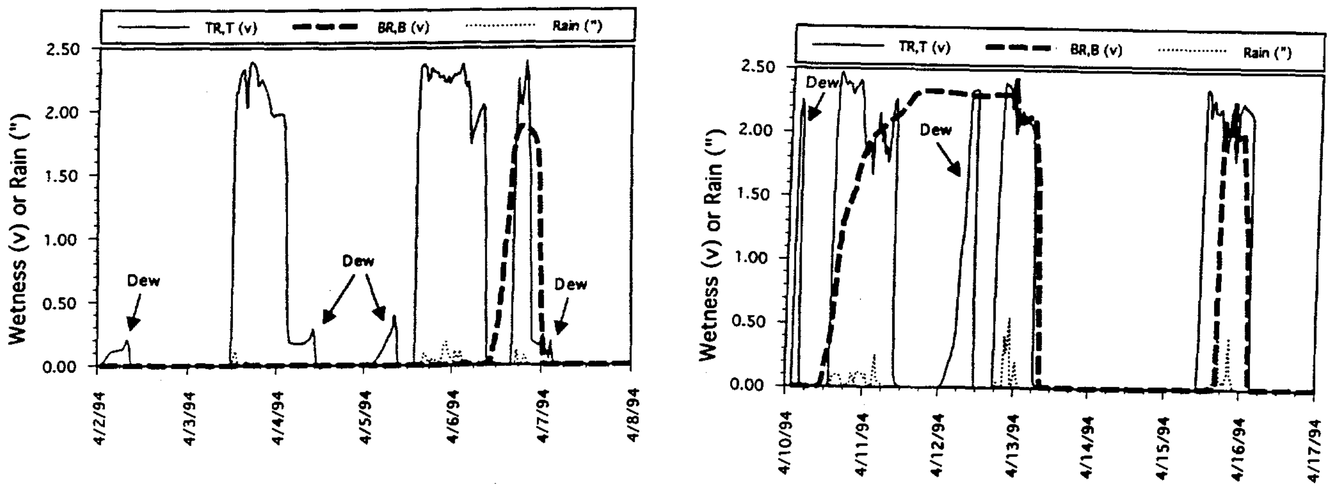

(a) (b)

Figure 4. (a) and (b) Wetness data from TR, T and BR, B sensors along with rainfall data collected during two time periods in April, 1994 at the K-south location.

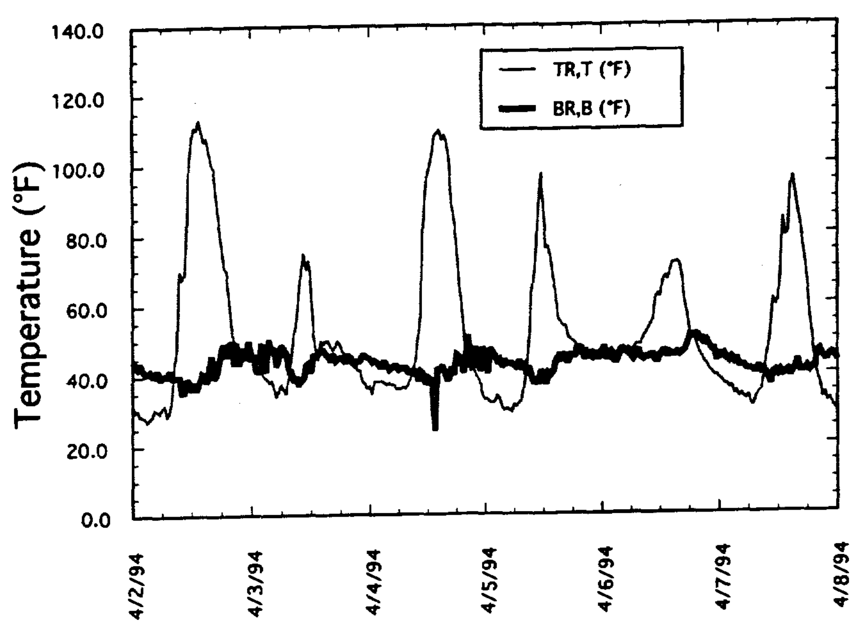

Figure 5. Surface temperature data from TR, T and BR, B surfaces at K-yard south for the same time period as Figure 4(a) showing much greater temperature fluctuations on TR,T surfaces due to radiative heating and cooling.

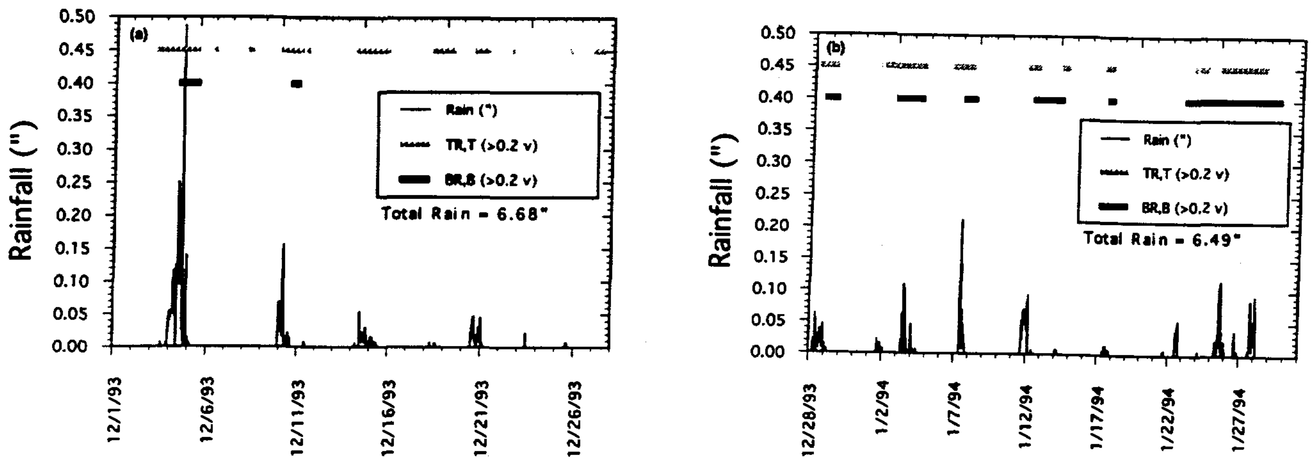

(a) (b)

Figure 6. (a) and (b) Rainfall data and periods over which TR, T and BR, B time-of-wetness sensors were 'on' during December 1993 and January 1994 at the E-yard location. The 'on' periods are shown as bars on top of the charts.

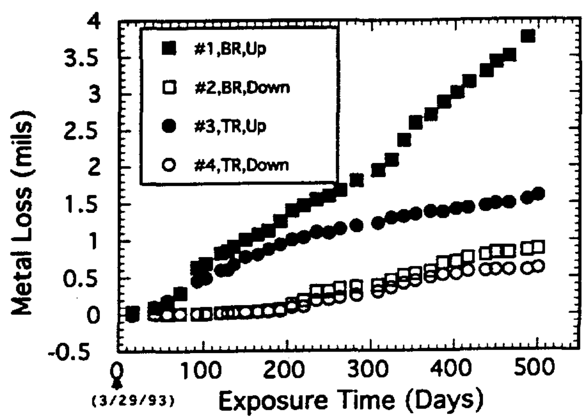

Figure 7. Typical corrosion probe data, for probes #1-4 mounted on cylinders at the K-north location.

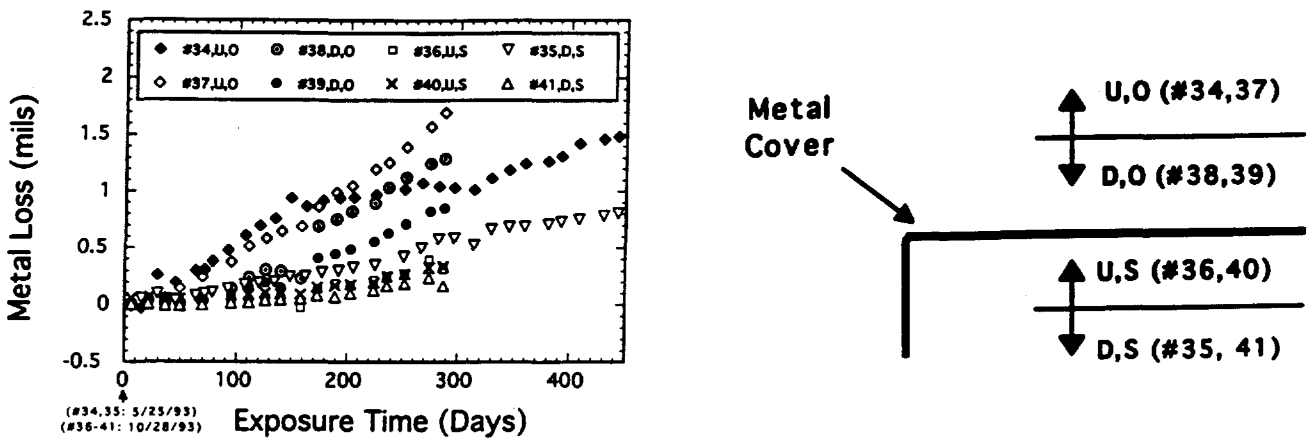

(a) (b)

Figure 8. (a) Corrosion probe data from probes installed in various orientations on the coupon rack in K-yard. (b) Schematic showing the orientations of probes. The arrows point in the direction the probe is facing. U, O = up, open; D, O = down, open; U, S = up, sheltered; D, S = down, sheltered.

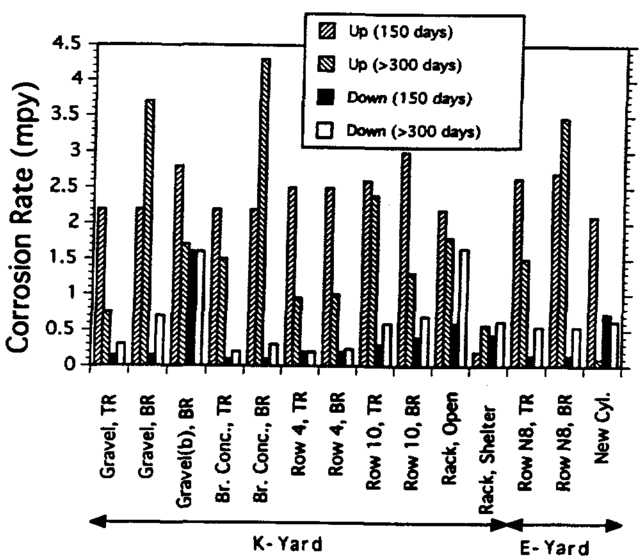

Figure 9. Corrosion rates calculated from data from corrosion probes.

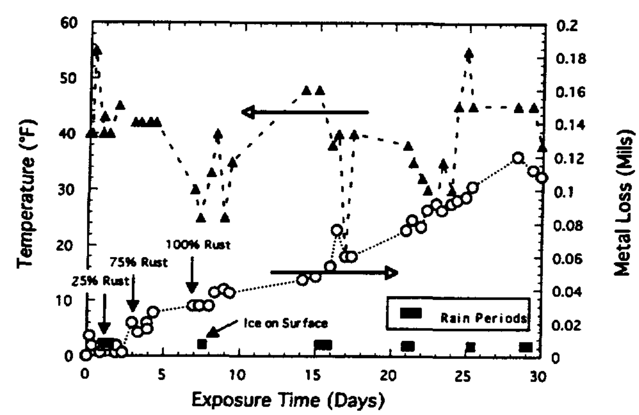

Figure 10. Data from probe #54 (mounted facing up horizontally) showing relationship between probe readings, periods of precipitation and ambient temperature.

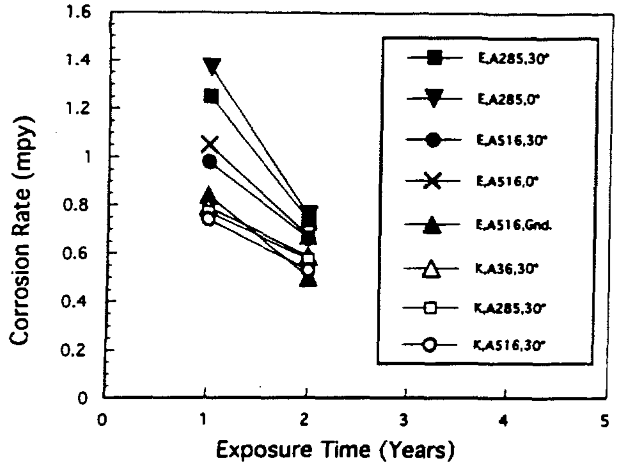

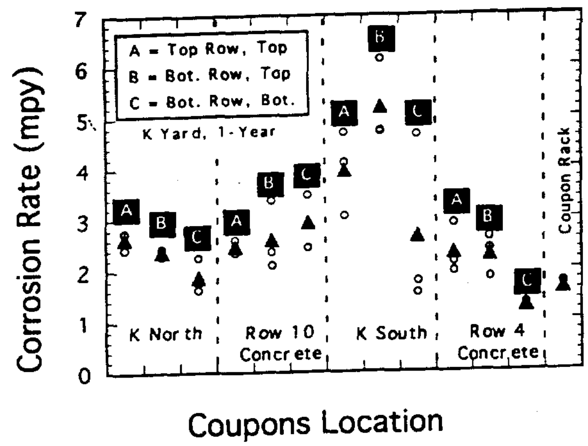

Figure 11. Corrosion rates measured after 1- and 2-years exposures from ASTM G50 type coupons (A36, A285 and A516 steels) mounted on coupon racks in E-yard and K-yard. Only average values are shown; the scatter in each data set was typically less than 10%.

Figure 12. Corrosion rates measured after 1 year exposure from A516 steel coupons mounted on cylinders in K-yard. (o = individual data points and Δ = average values.)

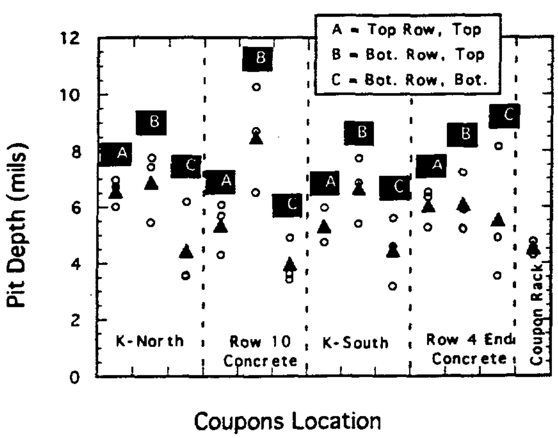

Figure 13. Results of pit depth measurements on A516 steel cylinder coupons after 1-year exposure showing consistently deeper pits on top-facing surfaces. Twenty of the deepest appearing pits were measured on each coupon and each data point corresponds to the average of the fifteen highest values. Compare data with Figure 12. (o = individual data points and Δ = average values.)